0273-2289/88/1800-0035/$03.40

Evaluation of O_2 and CO_2 Transfer Coefficients in a Locally Integrated Tubular Hollow Fiber Bioreactor

W. KANG, R. SHUKLA, G. T. FRANK,[a] AND K. K. SIRKAR*

Department of Chemistry and Chemical Engineering, Stevens Institute of Technology, Castle Point, Hoboken, NJ 07030; [a]currently at Merck Sharp and Dohme Research Laboratories, Rahway, NJ 07065

ABSTRACT

We have studied the transfer coefficients for O_2 transport to and CO_2 removal from a model cell-free system using microporous hydrophobic hollow fibers axially placed along a tubular bioreactor for ethanol production with immobilized yeast in the shell. In this locally integrated bioreactor, O_2 and CO_2 transfer rates depend strongly on the shell side liquid flow rate; O_2 flow rate in the fiber bore influences O_2 transport only at very low flow rates. Diffusion of CO_2 does not affect O_2 transport. Local and overall O_2 and CO_2 transfer coefficients have been determined for a wide range of Reynolds Numbers. The efficiency of such transfers has been demonstrated for alcohol fermentation.

Index Entries: Hollow-fiber; oxygen; carbon dioxide; transport; fermentation.

INTRODUCTION

Successful industrial fermentation processes require efficient supply of nutrients to and removal of metabolic products from the bioreactor. The bioreactor often has a high cell density, especially if immobilized microorganisms are being utilized or culturing of animal cells is performed. For aerobic fermentation processes and mammalian cell culture, adequate oxygen supply from the gas phase to the cells through the med-

*Author to whom all correspondence and reprint requests should be addressed.

ium is a challenging problem. Traditionally, oxygenation is achieved by sparging air coupled to a variable speed impeller. The energy costs are considerable because of high energy dissipation levels, gas compression, and so on. An earlier review of aeration is provided by Blanch (*1*).

Such conventional sparging-based oxygen supply processes can cause damage to shear-sensitive organisms (*2*). Should the fermentation media viscosity change during processing, the oxygen transport resistance may increase drastically unless countered by enhanced agitation. Further, the addition of defoamers can cause complications during downstream processing. In fact, some secondary metabolites of interest occur at concentrations around those of defoamers (a few g/L).

An attractive alternative to air sparging is to locally couple a membrane to the bioreactor for supplying oxygen. Whereas traditional nonporous gas separation membranes e.g., silicone, require a substantial partial pressure difference of oxygen across the membrane for oxygen transport, use of microporous hydrophobic membranes drastically reduces this requirement. The broth contacts the air or oxygen at the outer surface of the hydrophobic microporous hollow fibers (HMHF) through whose lumen oxygen or air is supplied. Simultaneously, carbon dioxide from the broth is transferred into the fiber lumen and removed by the gas stream. When the membrane pores are of appropriate size, the air or oxygen supplied need not be sterilized; the microporous membrane acts as a filter for bacteria. Frank and Sirkar (*3*) have recently demonstrated *in situ* gas exchange in a tubular immobilized yeast fermentor containing HMHF-s axially positioned for alcohol production.

Such a set of HMHF-s have bifunctional characteristics. Frank and Sirkar (*3*) have shown that at a later stage in the fermentation, the same set of hollow fibers used earlier for gas exchange could have a solvent flowing through the fiber lumen to extract fermentation products from the broth in a dispersion-free fashion. The *in situ* solvent extraction recovery of bioproducts using HMHF-s was demonstrated and studied earlier by Frank and Sirkar (*4*).

Such dispersion-free O_2 supply, CO_2 removal and product recovery using hydrophobic hollow fibers could be implemented in a variety of reactor configurations, e.g., fluidized bed(s) with immobilized or flocculating cells, conventional stirred tank systems or an external membrane device. Adoption of fluorocarbons used as artificial blood for oxygenation could add another dimension to this membrane-based immobilized interface solute exchange technique (*5–9*).

We have therefore undertaken a detailed characterization of the oxygen transport rate into the broth from the HMHF-s in a tubular fermentor. This has been done with pure water and substrate solution without fermentation in the presence or absence of carbon dioxide in the medium. The carbon dioxide stripping rates have also been measured. Quantitative estimates of oxygenation rate are analyzed in the context of recent correlations of shell side mass transfer coefficients in short micro-

porous hollow fiber devices (*7,10*). Whether the rates of O_2 transport and CO_2 removal are useful for alcohol production by yeast fermentation has been studied in the same bioreactor. These measurements provide a base condition for ongoing studies on nutrient supply and product removal in our hollow fiber bioreactor.

MATERIALS AND METHODS

Microorganism

The yeast used was *Saccharomyces cerevisiae* (NRRL Y-132), supplied by Northern Regional Research Laboratory (Peoria, IL). The composition of the medium was the same as that used by Gencer and Mutharasan (*11*). This medium was autoclaved and used for fermentation. Inoculum level was about 3% of total volume.

Fermentor-Extractor

A glass fermentor-extractor was used to carry out the fermentation. The fermentor-extractor (2.54 cm id, 128.3 cm long) is shown in Fig. 1. This consisted of six jacketed parts and five connecting parts having the sampling ports. These were joined with each other with pinch clamps, as shown in Fig. 1. This fermentor-extractor contained 295 hydrophobic microporous hollow fibers (Celgard X-20, Celanese Separations Products, Charlotte, NC) of 25.4 μm wall thickness and 240 μm internal diameter, running axially through the glass shell. The fiber ends were potted with Armstrong C-4D type epoxy (Beacon Chemical Co., Mt. Vernon, NY) to allow a solvent to pass through the fiber lumen without any mixing with the shell side broth. Separate openings were provided in the glass shell wall to introduce substrate flowing through the shell side packed with wood chips (2 × 5 mm, Forster Manufacturing Co., Wilton, ME). There was also an opening for inoculum. Five sampling ports were provided and besides these, there were openings at inlet and outlet. The fibers were checked for leakage before potting and defective fibers were discarded. After potting, the fermentor-extractor was checked again for leakage. It was found that one fiber was leaking; it was sealed with epoxy.

The experimental setup is shown in Fig. 2(a) and 2(b). The substrate and solvent, i.e., dibutyl phthalate (Aldrich Chemical Co., Milwaukee, WI) were delivered to the fermentor-extractor by means of 20 L pressure vessels (Sartorius GmbH, Gottingen, West Germany) as in Frank and Sirkar (*3*), using regulated nitrogen pressure source. These were collected in the receiving vessels with back pressure regulators controlling the pressure. Water at 30°C was circulated through the jackets surrounding the fermentor for maintaining constant temperature. The solvent was passed through an inline .2 μm membrane filter (Pall Corp., Vauxhall, NJ) to

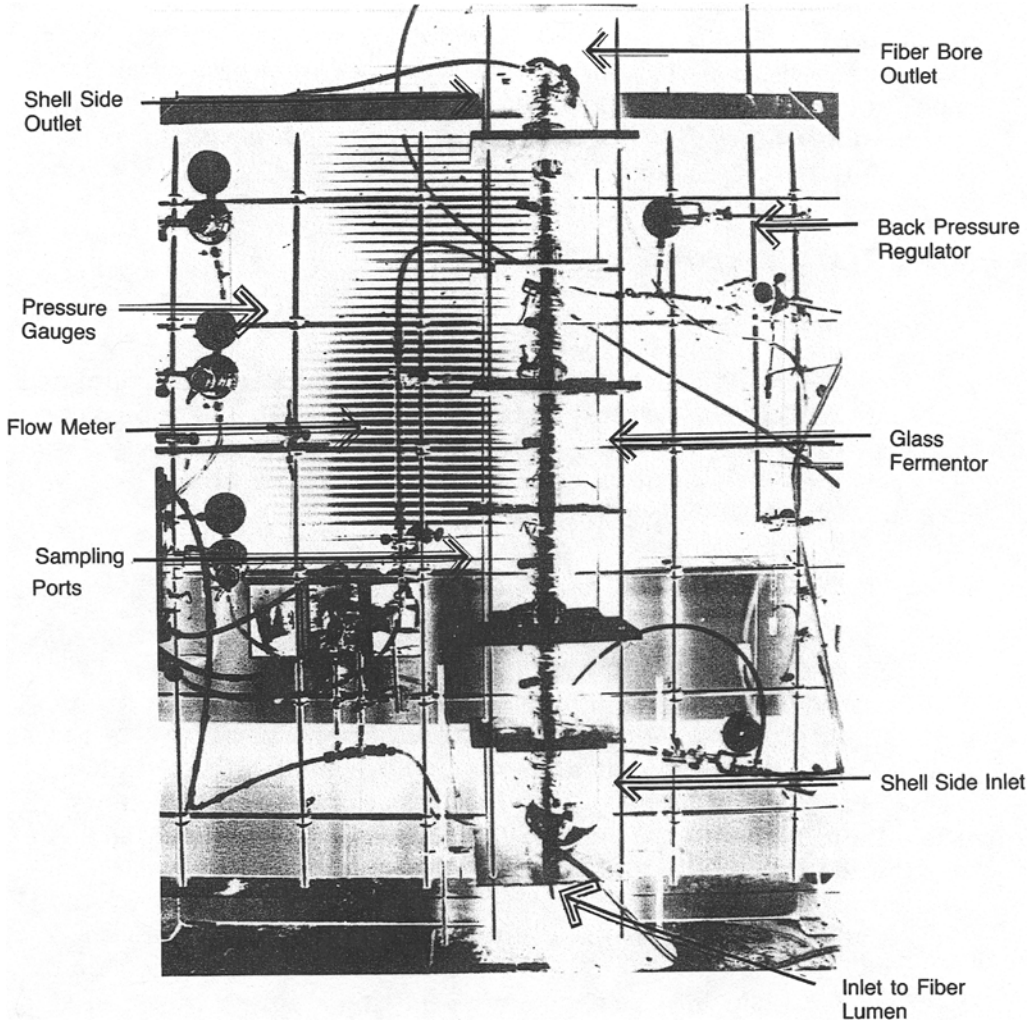

Fig. 1. Fermentor–Extractor.

avoid any possible fiber blockage caused by entrained solid impurities. Pure oxygen (Matheson, Rutherford, NJ) was used to supply oxygen to the fermentor.

Experimental Procedure

Oxygen was passed cocurrently through the fiber lumen and medium was passed through the shell side to study the oxygen transfer rate through the pores in the hollow fiber membrane to the medium. This was done before introducing wood chips into the shell side. Oxygen and medium flow rates were varied, one of them being constant in a given series of runs. Samples were taken out through the ports for dissolved oxygen analysis. The same set of experiments was repeated, with pure

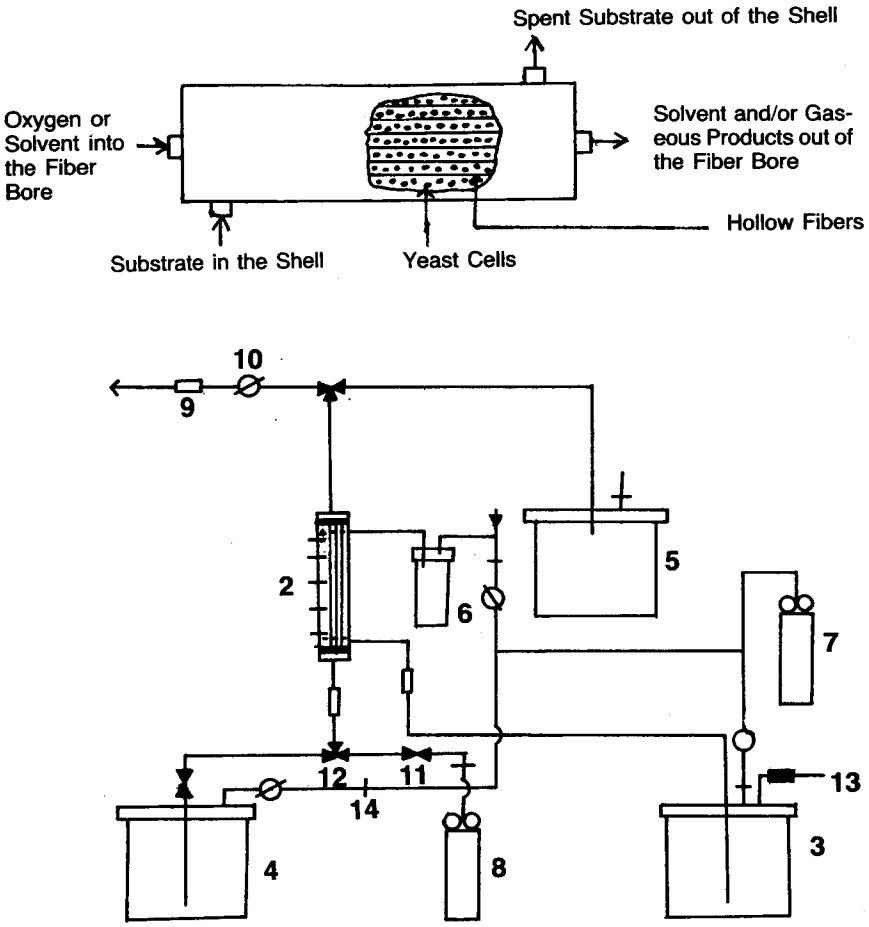

1) Tubular Fermentor/Extractor, **2)** Sampling Parts, **3)** Substrate Tank, **4)** Solvent Tank, **5)** Solvent Receiving Tank, **6)** Substrate Receiving Tank, **7)** Compressed Nitrogen, **8)** Compressed Oxygen, **9)** Flow Meters, **10)** Line Regulators, **11)** Valves, **12)** Three-Way Valve, **13)** Liquid Filter, **14)** Sterilizing Air Filter.

Fig. 2(a) and (b). Schematic diagrams of the setup.

water flowing through the shell side instead of the medium. In a separate series of experiments, carbon dioxide saturated medium was passed through the shell side to determine the effect, if any, of carbon dioxide on oxygen transfer through the pores to the medium. In these experiments, oxygen was passed through fiber lumen. The carbon dioxide content of the gas in fiber lumina was also monitored.

After these studies were completed, wood chips were introduced into the shell side. The fermentor-extractor was sterilized by passing ethanol (40%) through shell side for one hour and then sterile air was passed to dry the fermentor-extractor. Since ethanol (40%) wets the fiber and

subsequently appears on the tube side, there was no need to pass ethanol on the tube side. After sterilization, the medium was used to fill the fermentor and both ends were closed. This medium was then inoculated through all five ports with previously grown inoculum. Cells were allowed to grow for at least 20 h. Oxygen was then passed to facilitate cell growth. Fresh medium was passed continuously after cell growth until steady state was achieved. At this stage, solvent was allowed to pass through hollow fiber lumina to achieve solvent extraction of alcohol. The shell side pressure was kept higher than tube side so that solvent would not pass to the shell side. A constant pressure difference was always maintained. Samples were collected at different time intervals and analyzed for glucose, ethanol, oxygen, carbon dioxide, optical density, dry weight, and so on, as required.

Analytical Methods

Ethanol concentration was determined with a Hewlett Packard gas chromatograph (model 5890A) using a Porapak Q (80/100) column and a flame ionization detector. Carbon dioxide concentration in the gas phase was determined using the above GC with the same column using a thermal conductivity detector. Dissolved oxygen level was determined using a Harvard small volume oxygen uptake system (Harvard Biosciences, South Natick, MA). Carbon dioxide concentration in the liquid phase was determined using an ORION carbon dioxide electrode model 950200 (Orion Research Inc., Boston, MA) fitted into a Corning pH meter model 140 (Corning Glass Works, Corning, NY). The glucose concentration was analyzed by a glucose analyzer (YSI model 27). Cell growth was estimated by measurement of the optical density at 540 nm using Bausch and Lomb spectrophotometer model 1001.

RESULTS AND DISCUSSION

The results are presented and discussed under three sections: oxygen transport through water and medium, oxygen transport in medium saturated with carbon dioxide, and fermentation.

The local as well as length-averaged overall gas mass transfer coefficients were determined for both O_2 and CO_2. The following differential relations were utilized with z being the axial coordinate:

Mass balance at any section of fibers

$$Q_w \, dC_w/dz = K_{oz} \, \pi d_t n(C_w^* - C_w) \tag{1}$$

where

$$C_w^* = C_G/m_i$$

Overall mass balance

$$Q_w(C_{wo} - C_{wi}) = Q_G(C_{Gi} - C_{Go}) \quad (2)$$

In the above equations, Q_w and Q_G are the liquid and gas flow rates, C_{wo} and C_{wi} are exit and inlet concentrations of oxygen in liquid phase, C_{Gi} and C_{Go} are the inlet and outlet molar concentrations of oxygen in the gas phase, K_{oz} is the local oxygen mass transfer coefficient, d_t is the outer fiber diameter, n is the number of fibers, and m_i is Henry's constant for O_2. Similar relations are developed for CO_2 transport.

Rearranging Eqs. [1] and [2] and integrating K_{oz} along the length, we get an expression for the overall mass transfer coefficients K_{OA}.

$$K_{OA} = 1/\pi\, d_t n L\, [1/Q_w + 1/Q_G m_i]^{-1} \ln [C_{Gi}/m_i - C_{Go}]/[C_{Gi}/m_i - Q_w(C_{wo} - C_{wi})/m_i Q_G - C'_{wo}] \quad (3)$$

This equation was used to calculate the values of K_{OA}. These were also obtained from the correlations developed by Prasad and Sirkar (*7*) from solvent extraction and Yang and Cussler (*10*) from gas absorption.

Prasad and Sirkar (7)

$$K_{OA} = 5.8\ (D_i/L)(1 - \phi) N_{Re}^{.66}\, N_{Sc}^{.33} \quad (4)$$

Yang and Cussler (10)

$$K_{OA} = 1.25\ (D_i/d_e)\ [N_{Re}\, d_e/L]^{.93}\, N_{Sc}^{.33} \quad (5)$$

where D_i is the diffusivity, d_e is equivalent diameter, $(1 - \phi)$ is void fraction, L is the length of fibers, N_{Re} (Reynolds Number) is $d_e v/\upsilon$, N_{Sh} (Sherwood Number) is $K_{OA} d_e/D_i$, N_{Sc} (Schmidt Number) is υ/D_i, v is linear liquid velocity, and υ is kinematic viscosity of the liquid.

Oxygen Transport Through Water and Medium

The water flow rates and oxygen flow rates were varied over a wide range, keeping one of them as a constant. Figure 3 displays the O_2 concentration in water as a function of the fiber length at two different water flow rates for a constant tube side gas flow rate of .0727 cc/s. The temperature was 30°C. The saturation level concentration of O_2 in water is 10.458×10^{-7} mol/mL (*12*). It appears that at a water flow rate of .01333 mL/s, the exit stream is almost saturated in O_2. However, at a much higher flow rate of .11 mL/s, oxygen concentration increases slowly and does not rise up to the saturation level. At lower flow rates it appears possible to saturate the water with O_2 in the fermentor with the available number and length of fibers.

The Sherwood Number is plotted against the Reynolds Number in Fig. 4 for pure water flow. The same set of experiments was repeated

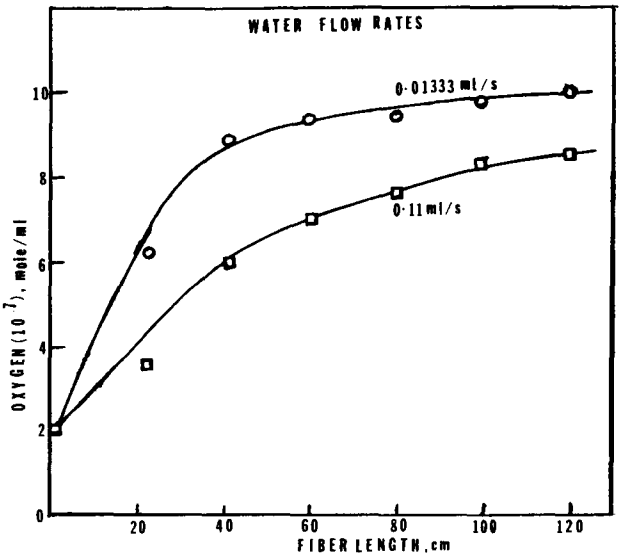

Fig. 3. Effect of shell side flow rate on oxygen transport into water. ○ Flow rate .01333 mL/s; □ Flow rate .11 mL/s.

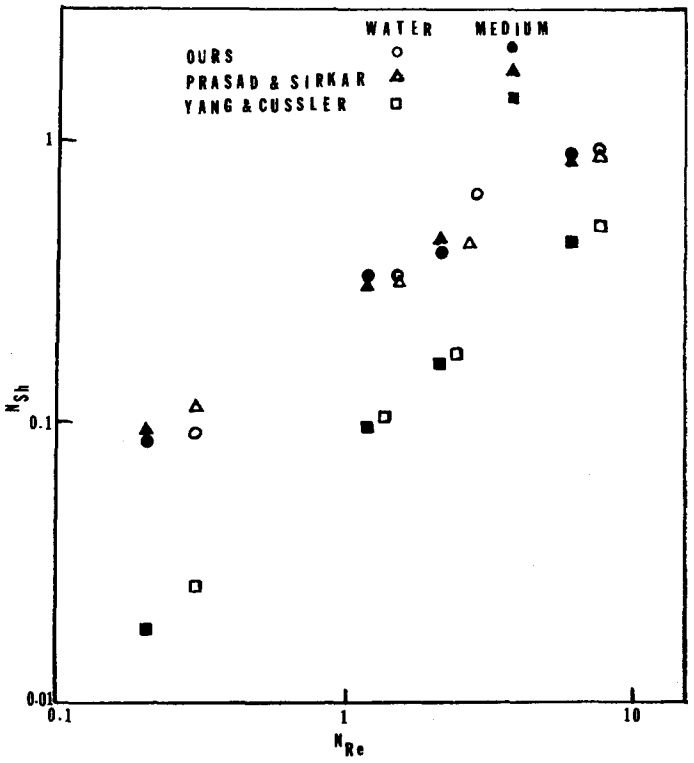

Fig. 4. Effect of shell side flow rate on overall Sherwood Number (log-log plot). ○ Data with Eq. [3] in water. ● Data with Eq. [3] in medium. □ Data with Yang and Cussler's correlation in water. ■ Data with Yang and Cussler's correlation in medium. △ Data with Prasad and Sirkar's correlation in water. ▲ Data with Prasad and Sirkar's correlation in medium.

with the medium. The flow rates were also kept identical. The tube side gas flow rate was kept constant at .0727 cc/s. In the same figure, N_{Sh} based on the overall mass transfer coefficients predicted by Prasad and Sirkar's (*7*) as well as by Yang and Cussler's (*10*) correlations are plotted. It can be noted that there is very little difference between the water and medium data. This holds for Eqs. [4] and [5] also. The viscosity of medium is about 1 cp; for water it is .795 cp at 30°C. The densities are also very close. Therefore, it seems logical that the overall mass transfer coefficients should not differ significantly. It is also useful to note that the experimental overall mass transfer coefficients calculated by Eq. [3] agree well with the coefficients obtained from Prasad and Sirkar's correlation.

The variation of overall mass transfer coefficients with shell side flow rates are shown in Fig. 5. The data are plotted in the manner of the Wilson plot (*13*). It appears that $(1/K_{OA})$ does vary with $Q_w^{-.66}$, as suggested by Prasad and Sirkar (*7*). When extended to very high flow rates $(Q_w^{-.66} = 0)$, $1/K_{OA}$ approaches zero, suggesting no membrane resistance or tube side resistance. The data for medium, also shown on the plot, suggests slightly higher resistance. In all these experiments, the gas flow rate was constant.

Tube side gas flow rates were also varied to determine any effect on the overall mass transfer coefficient. The flow rate in shell side of water

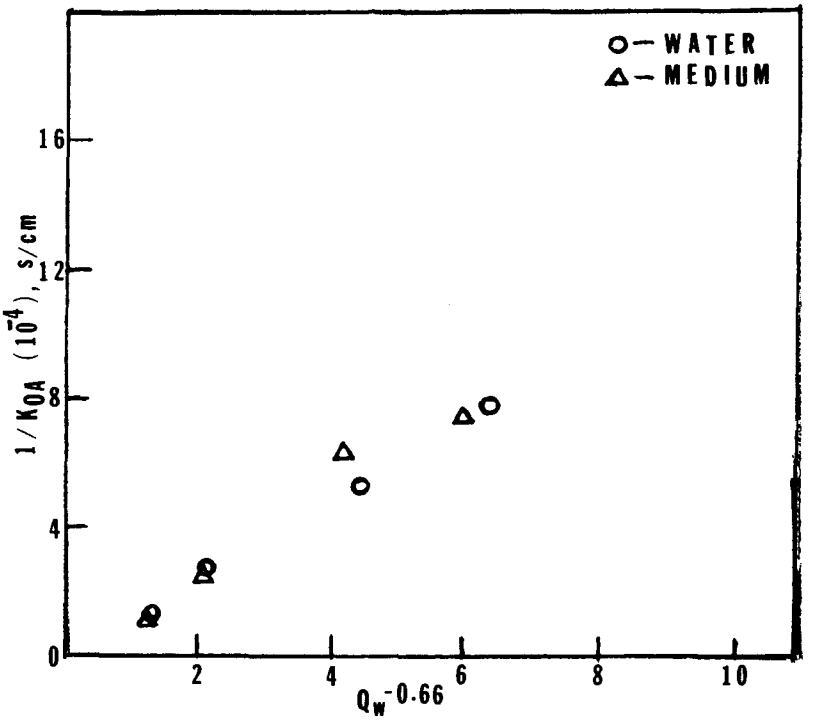

Fig. 5. Effect of shell side flow rate on overall oxygen mass transfer resistance. O Overall mass transfer resistance with water. Δ Overall mass transfer resistance with medium.

and medium was constant at .1067 mL/s. In the low flow rate range in the tube side, the overall mass transfer coefficient in the water does not vary significantly beyond a gas flow rate of 1 cc/s. A similar trend was observed also with the medium. These data (not shown here) indicate, as we observed earlier, that the mass transfer resistance on the tube side is very small and can be neglected. By resistance, we refer here to a pressure drop in oxygen on the tube side.

The overall N_{Sh} is plotted against the fiber length in Fig. 6. The results are also compared with the two correlations. These data are only for

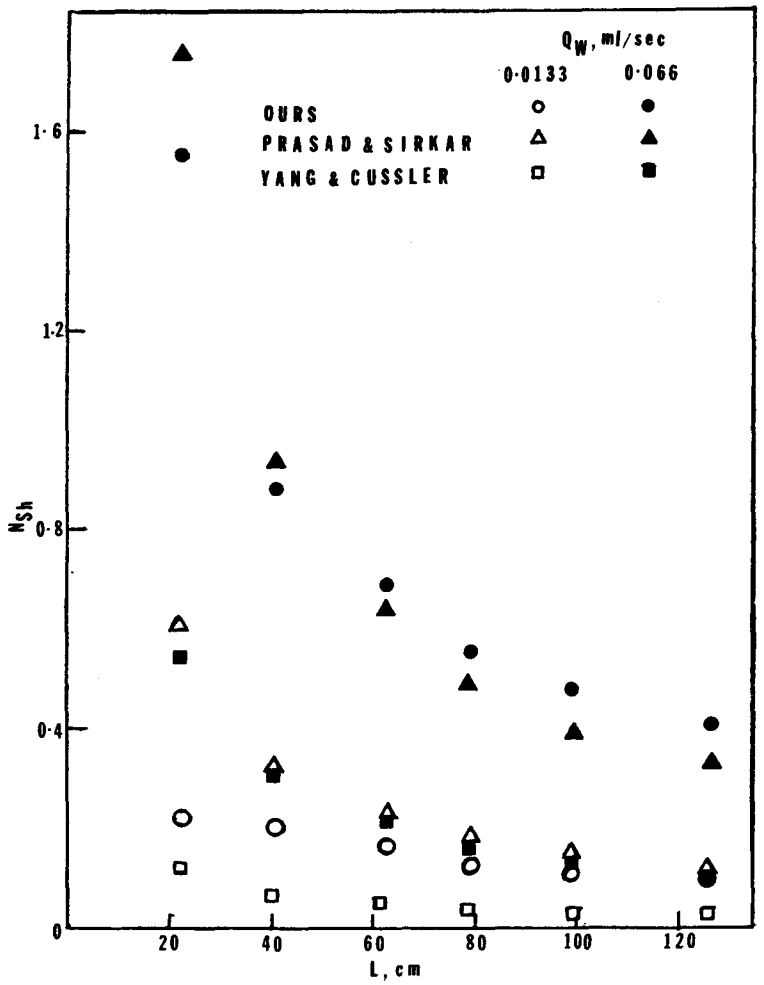

Fig. 6. Overall Sherwood Number variation with fiber length. ○ Data with Eq. [3] at .01333 mL/s flow rate. ● Data with Eq. [3] at .066 mL/s flow rate. △ Data with Prasad and Sirkar's correlation at .01333 mL/s flow rate. ▲ Data with Prasad and Sirkar's correlation at .066 mL/s flow rate. □ Data with Yang and Cussler's correlation at .01333 mL/s flow rate. ■ Data with Yang and Cussler's correlation at .066 mL/s flow rate.

water flowing through shell side. It appears that at the entrance of the fermentor, the flow is not fully developed in the shell side. The overall mass transfer coefficient decreases rapidly with the increase in length of fibers. This is self explanatory from the point of view of concentration boundary layer development (*14*).

The local mass transfer coefficient averaged over each section was calculated and plotted against length of fibers at different shell side flow rates in Fig. 7. The trend is similar to that of Figure 6. The concentration

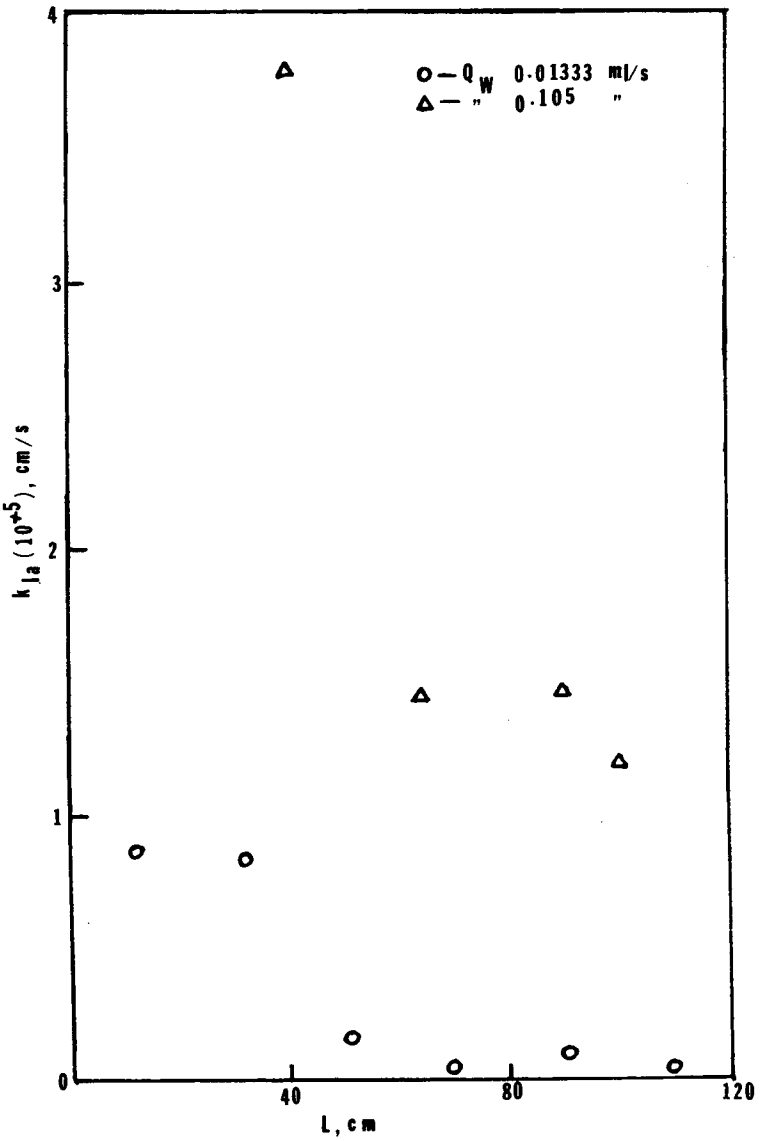

Fig. 7. Variation of local oxygen mass transfer coefficient with fiber length. O Shell side flow rate—.01333 mL/s. Δ Shell side flow rate—.105 mL/s.

profile and flow profile are not fully developed at the entrance of the fermentor. This is much more evident at the higher shell side flow rate. The local mass transfer coefficient decreases with increase in length, and the drop is much more significant at the entrance of fibers. We note further that the experimental coefficients obtained in this study agree within 10% with the coefficients calculated from Prasad and Sirkar's correlation.

Some comments are in order for oxygen transfer using either hydrophobic microporous hollow fibers or silicone membranes. The ability of silicone membranes to act as permselective barriers has been cited as a reason for utilizing them, rather than microporous membranes in oxygenating bioreactors, when air is being used as the gas supply. This is done in industrial settings, occasionally, for safety reasons. In those cases, it has been argued that the permselective membranes will enrich the air in oxygen, since the silicone is more permeable to oxygen than to nitrogen.

Under identical conditions, the broth phase resistance will be equal for both, i.e., silicone and microporous membranes. Hence, the overall resistance will differ only by the respective membrane resistances. In the case of the microporous membranes, oxygen diffuses through the gas, filling the membrane pores. In the worst case, we can assume that the pores are filled with nitrogen. The permeability will be equal to the diffusivity through the membrane times its solubility in the membrane (the latter being equal to one because of the membrane being essentially a gaseous mixture). Thus, for the microporous membrane, the permeability will be equal to the diffusivity of oxygen, which is approximately .2 cm^2/s. For silicone membranes, depending on the type of silicone rubber or copolymer and the extent of fillers used, the diffusivity may vary between 10^{-6}–10^{-7} cm^2/s. Hence, the great disparity of membrane resistances between microporous and silicone membranes is readily apparent.

Oxygen Transport in Carbon Dioxide Saturated Medium

In this set of experiments, the medium was saturated with carbon dioxide before passing through the fermentor to test whether the dissolved CO_2 concentration influences the oxygen transport into the medium. The N_{Sh} for O_2 is plotted against Reynolds Number with and without carbon dioxide saturation for medium in Fig. 8. There appears to be very little difference: CO_2 concentration does not have any significant effect on oxygen transport. We observe essentially similar behavior if we plot $1/K_{OA}$ against $Q_w^{-.66}$ for O_2 transport with or without CO_2 in the medium (Wilson plot). Note that the tube side flow rate was always constant at .0727 cc/s.

The N_{Sh} vs N_{Re} and $1/K_{OA}$ vs $Q_w^{-.66}$ for CO_2 and O_2 transport are shown in Figs. 9 and 10. In Fig. 9, the difference is not as distinct as it is in Fig. 10. It can also be noted that mass transfer resistance is smaller at

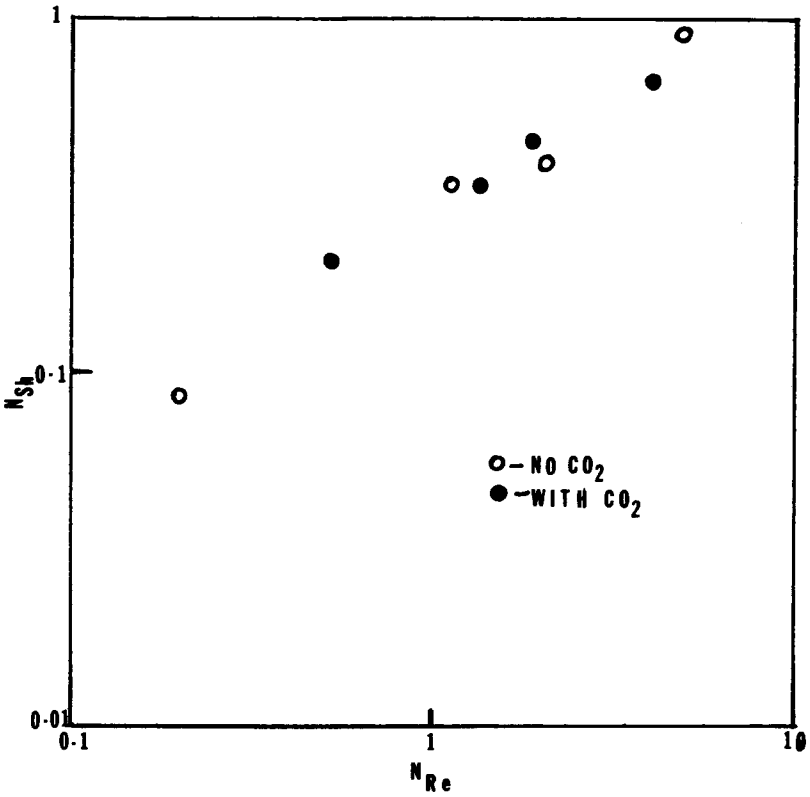

Fig. 8. Effect of carbon dioxide saturation in medium on oxygen Sherwood number (log-log plot). O Medium without carbon dioxide saturation. ● Medium with carbon dioxide saturation.

higher flow rates for oxygen transport than carbon dioxide transport. As expected, oxygen mass transfer coefficients are higher than that of carbon dioxide because of higher diffusivity in water.

Before we describe the fermentation experiments, we note that the 295 hollow fibers occupy only about 3% of the glass tubular reactor volume. We note further that at a shell side water flow rate of 4.22 mL/min and O_2 flow rate of .345 cc/min, the rate of O_2 supply was .051 gm/L/h. Obviously, the rate can be increased by increasing the number of fibers and reducing the fiber diameter (without increasing the fractional volume occupied by the fibers).

Fermentation

After the oxygen-transport experiments were completed in the tubular glass fermentor, fermentation runs were started with wood chips, introduced in the shell side. The shell side was filled with the medium and inoculum was introduced through the five ports at five different levels of fermentor. After a 16-h growth period, it was observed that the cell den-

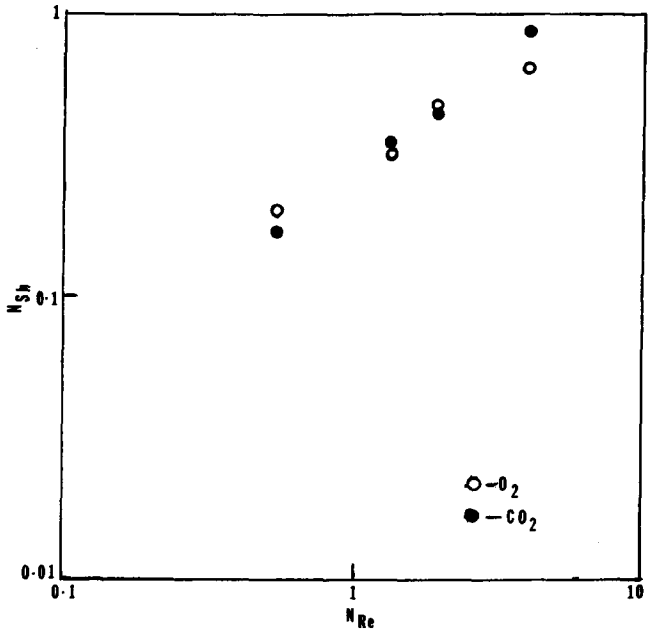

Fig. 9. Comparison of Sherwood Number against Reynolds Number for carbon dioxide and oxygen (log-log plot). ○ Medium without carbon dioxide saturation. ● Medium with carbon dioxide saturation.

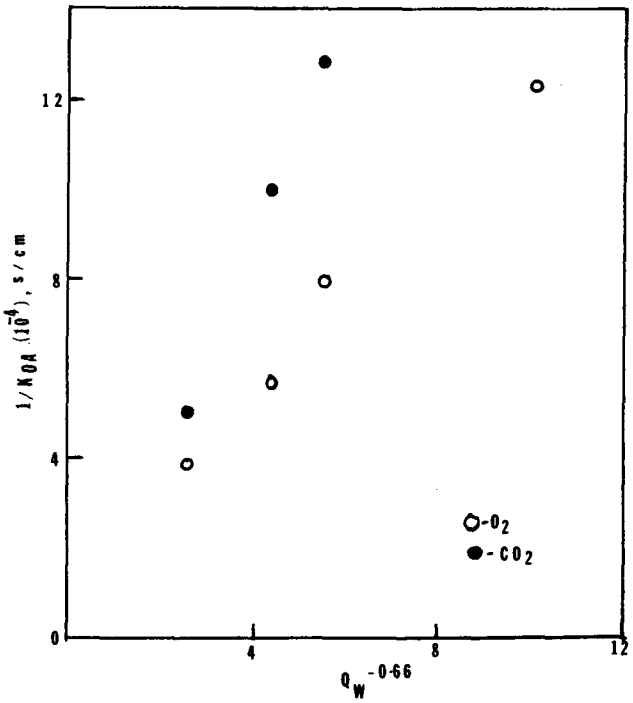

Fig. 10. Comparison of mass transfer resistance for carbon dioxide and oxygen. ○ Medium without carbon dioxide saturation. ● Medium with carbon dioxide saturation.

sity was low. The medium in the fermentor was inoculated again and cells were allowed to grow for another 20 h. At this time, regular medium was allowed to flow into the fermentor at a flow rate of 2 cc/min. The void volume inside fermentor exclusive of the fibers was 360 mL; thus the medium residence time was 180 min.

As the fermentation progressed, samples were withdrawn from all five ports along the fermentor and at the exit of the fermentor at suitable times. These results are shown in Fig. 11. It is obvious that even after 40

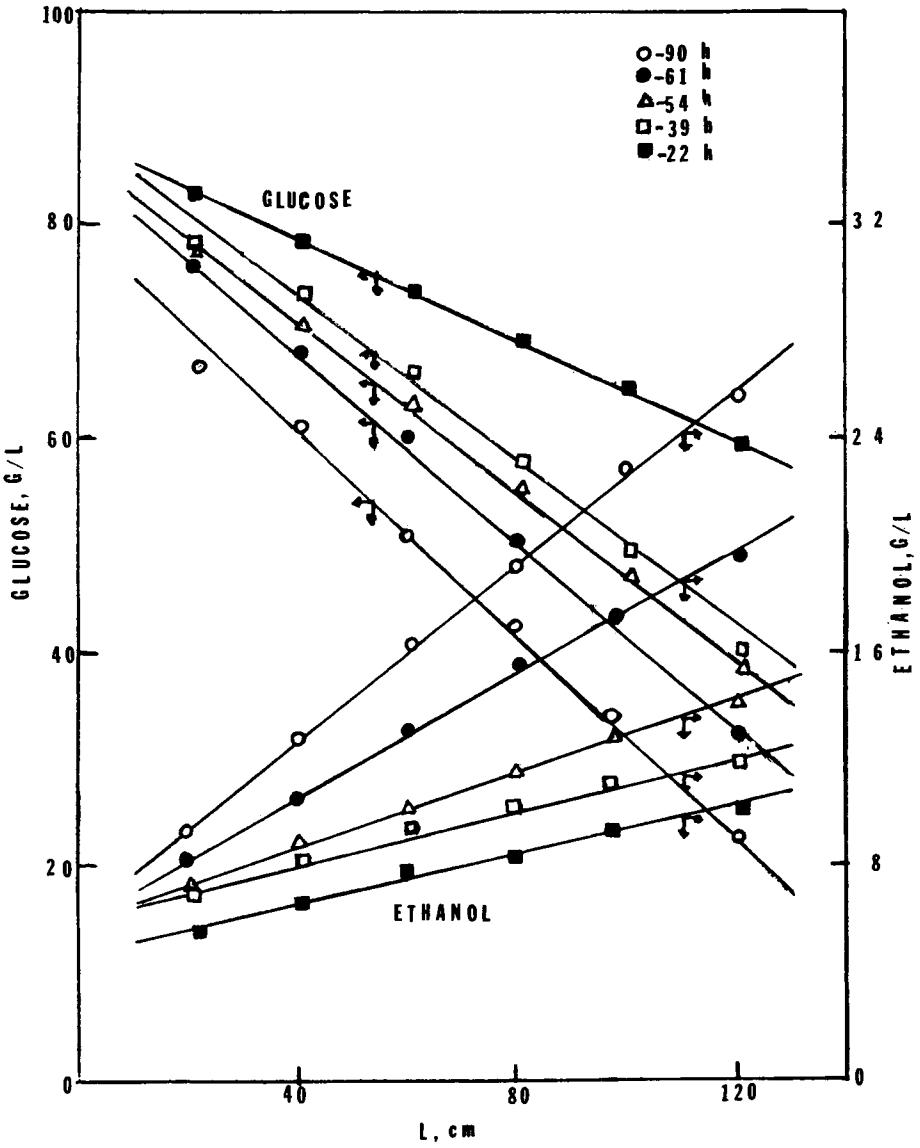

Fig. 11. Production levels of glucose and ethanol with fiber length. ○ Fermentation time 90 h. ● Fermentation time 61 h. △ Fermentation time 54 h. □ Fermentation time 39 h. ■ Fermentation time 22 h.

h of fermentation, the ethanol concentration in the broth was quite low. It is to be noted that fermentation time is counted from the instant, regular medium was allowed to flow. After 56 h of fermentation, oxygen was introduced into the fiber lumen to facilitate cell growth. Samples withdrawn at 61 h indicated an increase in ethanol concentration (Fig. 11) everywhere along the fermentor. Analysis of samples at 90 h indicated a further increase in alcohol concentration. At this time, the ethanol concentration was 26.7 g/L and the exit glucose concentration was 22.5 g/L. Oxygen flow was terminated. No further increase in ethanol concentration was observed.

This experiment indicates clearly the important role of air/oxygen in developing high initial cell concentration and thereby managing ethanol concentration in the broth (*15*). We notice further that the ethanol concentration increase with the shell length is linear implying uniform cell growth along the fermentor. The linear decrease in glucose concentration along the fermentor length further supports the hypothesis. We did not observe any washout in the fermentor substrate exit stream.

Concentrations of glucose and ethanol at the fermentor outlet are plotted against time in Fig. 12. Predictably, glucose concentration de-

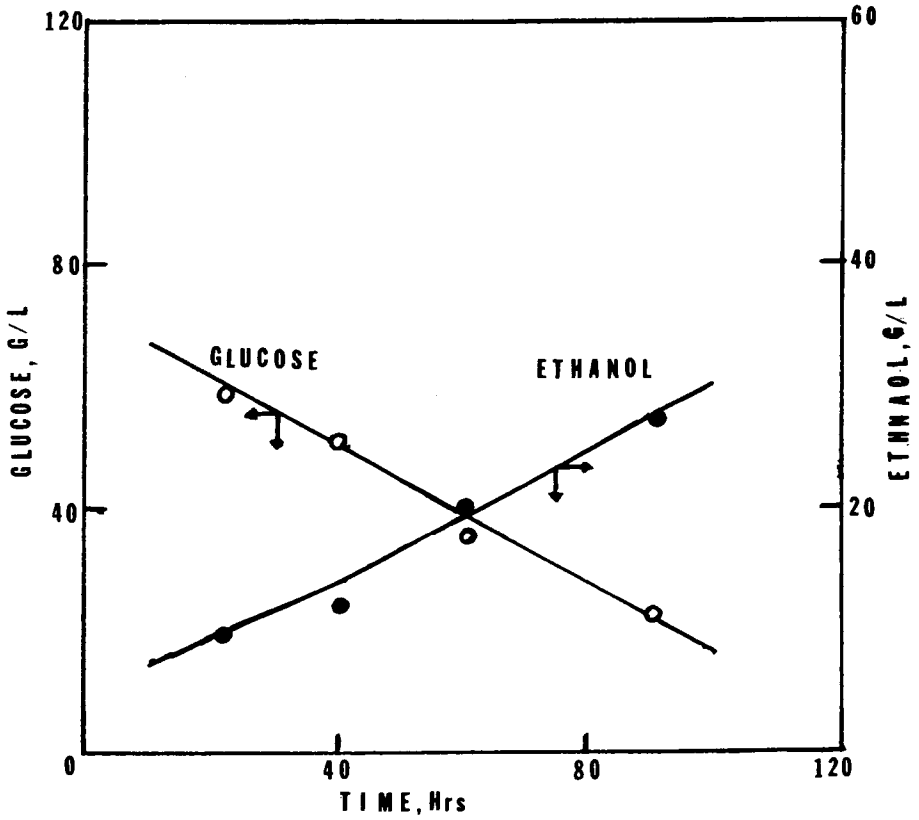

Fig. 12. Exit glucose and ethanol concentrations with time. ○ Glucose concentration. ● Ethanol concentration.

creased with time while that of ethanol increased with time. The exit stream was not recycled. Further details on fermentation experiments with and without solvent extraction will be communicated elsewhere.

ACKNOWLEDGMENTS

The authors thank New Jersey Commission on Science and Technology for providing partial funding for the project under the Biotechnology Initiative of the Innovation Partnership Program. G. T. Frank was awarded a LINK Energy Fellowship to carry out part of this investigation. We would also like to acknowledge Questar Inc., Charlotte, NC for their generous supply of Celgard hollow fibers.

REFERENCES

1. Blanch, H. W. (1979), *Annual Reports on Fermentation Processes,* Academic, New York, **3,** 47.
2. Tolbert, W. R., Schoenfeld, R. A., Lewis, C., and Feder, J. (1982), *Biotechnol. Bioeng.* **24,** 1671.
3. Frank, G. T., and Sirkar, K. K. (1986), *Biotechnol. Bioeng. Symp.* **17,** 303.
4. Frank, G. T., and Sirkar, K. K. (1985), *Biotechnol. Bioeng. Symp.* **15,** 621.
5. Kiani, A., Bhave, R. R., and Sirkar, K. K. (1984), *J. Membrane Sci.* **20**(2), 125.
6. Prasad, R., Kiani, A., Bhave, R. R., and Sirkar, K. K. (1986), *J. Membrane Sci.* **26**(1), 79.
7. Prasad, R, and Sirkar, K. K. (1986), *Dispersion-Free Solvent Extraction with Microporous Hollow Fiber Modules,* presented at A.I.Ch.E. Summer National Meeting at Boston, MA, *AIChE J.* (1988), in press.
8. Prasad, R., and Sirkar, K. K. (1987a), *Sep. Sci. and Tech.* **22**(2,3), 619.
9. Prasad, R., and Sirkar, K. K. (1987b), *AIChE J.* **33**(7), 1057.
10. Yang, M., and Cussler, E. L. (1986), *AIChE J.* **32,** 1910.
11. Gencer, M. A., and Mutharasan, R. (1983), *Biotechnol. Bioeng.* **24,** 2243.
12. Perry, J. H. (1973), *Chemical Engineering Handbook,* 5th ed., McGraw Hill, New York, 3–18.
13. Wilson, E. E. (1915), *Trans. ASME* **37,** 47.
14. Skelland, A. H. P. (1974), *Diffusional Mass Transfer,* Wiley, New York, 164.
15. Ryu, D. D. Y., Kim, Y. J., and Kim, J. H. (1984), *Biotechnol. Bioeng.* **26,** 12.